

Effect of a crack on strength of fibre-reinforced plastics

S. L. BAZHENOV, A. A. BERLIN

Institute of Chemical Physics, Academy of Science of the USSR, Kosigin Street, 4, 117 977 Moscow, USSR

In unidirectionally reinforced composites with an elastic-plastic matrix, there is a plastic zone with length γ_0 proportional to the crack length C ($\gamma_0 \gg C$) at the tip of a crack. This results in a new logarithmic dependence of glass and aramid PABI fibre-reinforced plastics (FRP) on crack length and non-fulfilment of the Griffith criterion. In glass and PABI FRP without an artificial notch, defects already exist equivalent to a crack with a length depending on composite fabrication practice. In GFRP, the epoxy matrix shear yield stress grows 2.0 to 2.5 times, compared to the yield in thin films due to fibre constraint of matrix yielding. The stress distribution in front of a crack in a highly anisotropic composite with an elastic-plastic matrix is derived. The stress concentration at the tip of a crack grows with increasing matrix yield stress, resulting in a change of failure mode from accumulation of fibre breaks at low matrix strength, to brittle failure at high matrix strength. The following factors lead to composite embrittlement: (1) increase of matrix yield stress and composite shear strength; (2) decrease of temperature; (3) increase of Young's modulus of the fibre; (4) reduction of fibre strength. The dependence of aramid PPTA FRP strength on temperature exhibits a maximum. Epoxy matrix plastification leads to some increase of aramid PPTA FRP strength.

1. Introduction

One of the major problems of fracture mechanics is the influence of stress concentrators on strength. Using the solution of Kolosov-Inglis [1] for stress distribution in an elastic isotropic body with a crack, Griffith introduced a thermodynamic criterion of fracture [2] which was successfully used for locally elastic-plastic metals and polymers. Application of linear fracture mechanics and Griffith criterion to the fibre-reinforced plastics encountered some difficulties, the most important of which are:

1. the strength does not decrease as sharply as is described by the Griffith criterion [3, 4];
2. the strength decreases if the radius of a circular hole is increased despite the independence of the stress concentration coefficient in the vicinity of the hole on its radius [3-6];
3. composite strength practically does not depend on the stress concentrator shape. For example, the strength dependences on crack length and hole diameter coincide [3-5];
4. a notch oriented orthogonally to the fibres may grow not in the initial direction but may turn 90° and grow along the fibre direction [7, 8].

Many attempts have been made to modify the linear fracture mechanics in order to solve these problems. The modification of fracture mechanics was realized in two main ways. The first is associated with the introduction of an empirical length parameter to describe the size of the fracture zone in front of a crack. A review of these works is presented in [4]. The main

shortcoming of this method is the not very good agreement between theory and experimental data over a wide enough range of crack lengths [9]. For example, a ten-fold increase in crack length leads to an approximately three-fold growth of empirical length parameter [10] which is really not constant. For this reason, other ways should be sought to solve the problem.

The second method of fracture mechanics modification describes the dependence of strength on the crack length by a power function with the index not equal to $-1/2$ [5, 6, 11]. The index of the power in this case is an empirical parameter, as well as the second constant, which is analogous to fracture toughness in classical fracture mechanics. The power function satisfactorily fits the experimental data. Unfortunately, the power index is not invariant for different composites and it cannot be predicted theoretically from fibre and matrix properties.

The present paper represents an attempt to create a fracture theory for composites with an elastic-plastic matrix, which is based on the solution for stress distribution in front of a crack in a highly anisotropic material with an elastic-plastic matrix. This solution principally differs from that of Kolosov for an elastic isotropic body, but it is analogous to the solution which was obtained in an unpublished work by McClintock [12] and used by Scop and Argon [13] to obtain stress concentration coefficients for the fibres in the tip of a crack. In the present paper the influence of a crack, oriented orthogonally to the direction of

reinforcement on the strength of unidirectional aramid and E-glass fibre-reinforced plastics is investigated.

2. Materials and experimental procedure

For reinforcement, aramid polyparaamidobenzimidazol (PABI) and polyparaphenilenterephthalamid (PPTA) fibres were used [14, 15]. Unless stated to the contrary, the matrix is epoxy EDT-10 resin which is a composition consisting of 80 parts by weight epoxy ED-20 (4,4'-bisglycidyl-bisphenol-A) resin, 10 parts modifier DEG (diethylene glycol) and 10 parts curing agent TEAT (triethanolaminetitanate). The matrix was cured at 160°C for 4 h.

We were especially interested in the influence of short cracks, but we were unable to obtain notched samples with artificial crack of length 40 to 100 μm, so hybrid samples consisting of three layers were tested. Fig. 1 shows the cross-section of the samples. Layers 1 and 3 in Fig. 1 are the investigated materials; layer 2 is of lower elongation fibres. During loading, the low elongation layer 2 is fractured, a crack appearing before the fracture of layers 1 and 3, which are sufficiently tough to arrest a running crack originating in layer 2. By varying the thickness of layer 2, we changed the crack length and investigated the fracture elongation and strength of the material. The thickness of layer 2 was measured in an optical microscope on a polished surface of the rings after testing.

Ring samples were made by winding filaments preimpregnated with resin. Layers 1, 2 and 3 were consequently wound on a mandrel 150 mm diameter and the matrix was subsequently polymerized. To investigate the strength of glass fibre-reinforced plastic we used plastics reinforced with aramid PABI and PPTA fibres as a low elongation layer 2 (the critical elongation of glass, PABI and PPTA fibres is 3.8 to 4.0, 3.1 to 3.3 and 2.4 to 2.6%, respectively). In order to investigate PABI fibre-reinforced plastic as layer 2, plastic reinforced by PPTA fibres was used.

The condition $C \ll B$ (Fig. 1) was always fulfilled. The crack could thus be considered in one dimension with a length C . For each measurement, five ring samples were tested using two joined half-discs [16].

Apart from ring samples, the tensile strength of strands, i.e. samples in the form of fibre bundles which are fixed by epoxy matrix in the exact position of preferred orientation, was also measured. To manufacture the strands, a bundle of liquid-matrix-impregnated fibres was wound on two different types of mandrel. The first was a cylinder, 350 mm diameter.

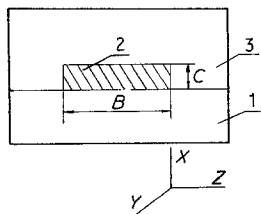


Figure 1 Cross-section of the sample. Layers 1 and 3, investigated material; 2, fibre-reinforced plastic with lower fracture elongation (layer 2); C , thickness of the layer 2; B its width. After fracture of layer 2, C is the crack length.

Owing to the axial pretension of the fibres on the round mandrel, transverse stresses arose and the strand cross-section became flat. The width of organic fibre strand was 1.5 to 2.0 mm with a maximum thickness of only 0.15 to 0.20 mm.

On the second mandrel the filament was not in contact with its surface over the work length, and transverse stresses did not appear. The strand cross-section in this case was practically round, and 0.3 to 0.35 mm diameter. To lower the stress concentration near the grips, the board straps were glued to the ends of strands. The strand gauge length was 100 mm. The matrix content in the strands was not less than 60 vol % to eliminate its longitudinal cracking. The strand strength was calculated from fibre area only, and the matrix cross-section was not taken into account.

Composite shear modulus was measured by torsion of unidirectionally reinforced tubes.

Mechanical measurements were carried out on "Instron 1122" and "Instron 1169" testing machines. Yield-zone length measurements were made with a "Karl Zeiss" optical microscope specially equipped with two polarizers.

3. Results

3.1. The effect of a crack on composite strength

Fig. 2 shows the dependence of glass fibre-reinforced plastic strength on crack length, C . This dependence may be presented as a straight line on semilog coordinates, $\sigma - \ln C$, the tangent of slope, q , is equal to 0.14

$$\sigma = \sigma_0 [1 - q \ln (C/C_0)] \quad C \geq C_0 \quad (1)$$

where σ_0 is the strength of the composite with no artificial notch.

The dependence may also be presented as a straight line using $\ln \sigma - \ln C$ coordinates (Fig. 3). Consequently, the composite strength may be described by a power function

$$\sigma = \sigma_0 / (C/C_0)^Q \quad (2)$$

where the power index Q is very close to the coefficient in front of the logarithm in Equation 1.

Fig. 4 shows the dependence of the PABI fibre-reinforced plastic strength on the crack length. A log dependence of composite strength is also observed, and the tangent of slope equals 0.06. C_0 depends on the plastic manufacture technology, and is approximately 40 μm if the composite is wound using a single filament, and 150 to 200 μm if it is wound as a roving consisting of 17 parallel filaments (curve 2, Fig. 4).

In accordance with Figs 2 and 4, a ten-fold increase

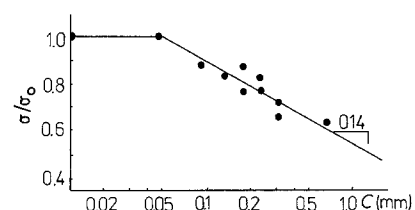


Figure 2 Strength, σ , against log (crack length, C) for glass fibre-reinforced plastic rings.

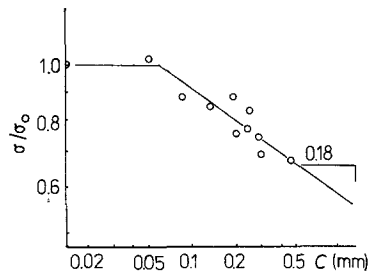


Figure 3 Log (strength) against log (crack length) for glass fibre-reinforced plastic.

in a crack length leads to decrease in organic and glass fibre-reinforced plastics strengths of not $10^{1/2}$ times, but of 14% and 32% only. The power indices are different for organic and glass fibre-reinforced plastics and it is lower in the case of organic fibre-reinforced composite. Thus, q defines composite sensitivity to defects. The higher the value of q , the higher is plastic sensitivity to defects.

The strength of a brittle material depends on the stress concentration in the vicinity of the most "dangerous" defect, consequently Figs 2 and 4 suggest that in a composite with no artificial notch, there is a stress concentrator equivalent to a crack of length C_0 . Note that a crack $50 \mu\text{m}$ long represents five or six rows of broken glass fibres (8 to $10 \mu\text{m}$ diameter) if the reinforcement content is approximately 60 vol %. Analogously, cracks 40 and 150 to $200 \mu\text{m}$ long present 3 and 12 to 15 rows of broken organic fibres which are 12 to $14 \mu\text{m}$ diameter.

Thus, we may draw some preliminary conclusions.

1. If the crack length is $< 1 \text{ mm}$, the strength of unidirectional glass and organic fibre-reinforced plastics does not decrease in accordance with the Griffith criterion, but logarithmically.

2. At the same time, if the crack length C is less than C_0 , no decrease in strength occurs. Consequently, in fibre-reinforced plastic with no artificial notch, there is already a stress concentration equivalent to a crack of length C_0 . The size of the composite defect C_0 depends on its manufacture technology.

3.2. Solution for stress distribution in front of a crack

To explain the log dependence of composite strength on crack length, the problem of stress distribution in front of a crack in a highly anisotropic reinforced material with an elastic-plastic matrix will be solved.

Note that epoxy matrix is elastic and brittle only in

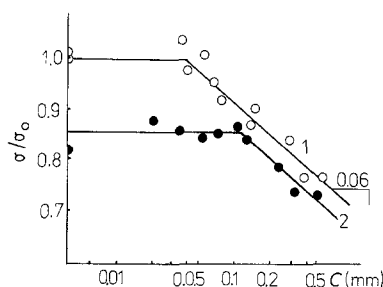


Figure 4 Strength against log (crack length, C) for aramid PABI fibre-reinforced plastic. Rings were wound from a single filament (1) and from a roving composed of 17 parallel filaments (2).

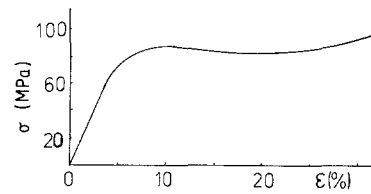


Figure 5 Stress-strain curve obtained for EDT-10 resin film $150 \mu\text{m}$ thick.

bulk, although the beginning of EDT-10 plastic deformation under tension is observed even in dog-bone shaped samples of 5 mm diameter [17], the critical elongation of which reaches 8 to 10%. The elongation of a resin film thickness of $150 \mu\text{m}$ reaches 30% to 40% (Fig. 5). Despite the composite elasticity on a macroscopic level, a matrix local plasticity is revealed near broken fibres and cracks in the composite (Fig. 6). Figs 5 and 6 show that the epoxy matrix may be considered as locally elastic-plastic.

Let us estimate the stress distribution in a unidirectionally reinforced composite after the material near the stress concentrator reaches yield stress. Everywhere except for this zone material is considered to be elastic. With this aim, we consider the elasticity theory problem for a half-plane with a tension stress, σ_0 , far from the crack. Reduction to the plane stress problem is justified because the crack length in the axial Z direction is an order higher than that in the axial X direction (Fig. 1).

If a crack is absent, then due to symmetry, the following conditions are satisfied

$$\tau|_{x=0} = 0, \quad S = S_0, \quad \sigma = \sigma_0$$

where τ is the shear stress, S the displacement, σ the tensile stress.

Let us suppose that a crack perpendicular to the direction of reinforcement appeared in the vicinity of $X = 0$ (Fig. 7). This leads to the appearance of a yield zone with a length y_0 parallel to the fibres. Let us

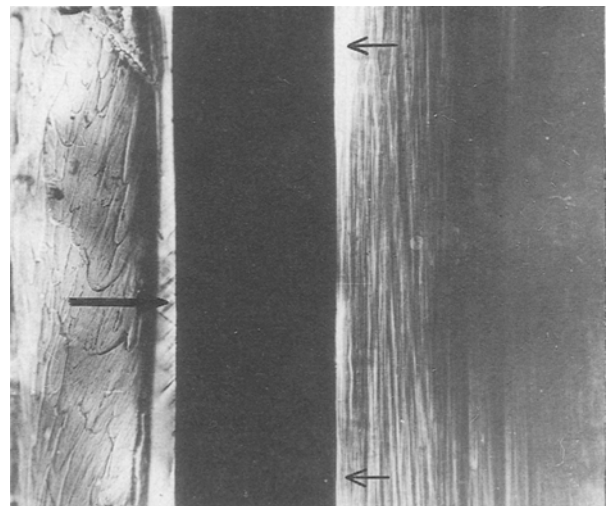


Figure 6 Photograph of the cracked area (polarized light). Arrows indicate shear lines in the epoxy resin in front of a crack, plastic zone oriented along the fractured carbon fibre-reinforced plastic (black zone) and overstressed area in the glass fibre-reinforced plastic. No crack in the carbon fibre-reinforced material is seen because carbon fibres are broken in different planes. The crack plane is analogous to a brush with sticking out fibres.

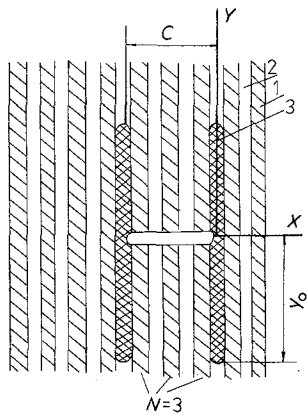


Figure 7 Model of composite with a crack. 1, fibre layer; 2, matrix layer; 3, yield zone in matrix. Three fibre layers are fractured. The composite, with the exception of yield zones, is assumed to be elastic in all areas.

assume that in this zone and in particular at $X = 0$, $-y_0 \leq y \leq y_0$ tangent stresses are equal to matrix yield limit. The length of the yield zone may be calculated from the equation, which results from the equilibrium of the cracked layer in shear lag approximation [18]

$$y_0 = C \sigma_0 / 2\tau_0 \quad (3)$$

where τ_0 is the matrix shear yield limit and σ_0 is the external tensile stress.

The influence of normal stresses on the boundary $X = 0$, as shown by additional analysis, may be neglected because normal stresses do not exceed the yield limit of the matrix. Strain hardening of the matrix in the yield zone is not taken into account.

Material in the half-plane $X > 0$ is considered to be highly orthotropic; then using the asymptotic method [19] and assuming $\alpha = G_c/E_c$ is small, we obtain in a first approximation the following boundary problem for the additional displacement $S(x, y)$ which is due to the existence of a disturbed zone (G_c and E_c are the composite effective moduli in shear and tension)

$$E_c \frac{\partial^2 S}{\partial y^2} + G_c \frac{\partial^2 S}{\partial x^2} = 0 \quad (4)$$

$$G_c \frac{\partial S}{\partial x} \Big|_{x=0} = \begin{cases} \tau_0 & \text{if } 0 \leq y \leq y_0 \\ -\tau_0 & \text{if } -y_0 \leq y < 0 \\ 0 & \text{if } |y| > y_0 \end{cases} \quad (5)$$

$$G_c \frac{\partial S}{\partial x} \Big|_{R \rightarrow \infty} = 0; \quad S \Big|_{R \rightarrow \infty} = 0$$

where $G_c(\partial S/\partial x)$ is the shear stress, Y the axis of fibre orientation, $X = 0$ the plane of the crack and $R = (x^2 + y^2)^{1/2}$.

Applying the Fourier transformation along coordinate y to Equation 4 and to the boundary conditions (Equation 5), we have

$$G_c \frac{d^2 V}{dx^2} - E_c t^2 V = 0 \quad (6)$$

$$G_c \frac{dV}{dx} \Big|_{x=0} = \frac{2i\tau_0}{t} (1 - \cos ty_0)$$

where $V(x, t) = \int_{-\infty}^{\infty} S(x, y) \exp(i ty) dy$.

The solution of Equation 6 under the requirement $V \rightarrow 0$ at $R \rightarrow \infty$ may be written in the following form

$$V(x, t) = \frac{2i\tau_0}{t|(E_c G_c)^{1/2}} (1 - \cos ty_0) \times \exp[-(E_c/G_c)^{1/2}|t|x] \quad (7)$$

Then the additional tensile stress is found to be

$$\sigma_y = E_c \frac{\partial S}{\partial y} = \frac{E_c i}{2\pi} \int_{-\infty}^{\infty} t V \exp(-ity) dy \quad (8)$$

Solving Equation 8 we have

$$\sigma_y = \frac{2\tau_0}{\pi} (E_c/G_c)^{1/2} \times \ln \left\{ 1 + \frac{C^2 \sigma_0^2}{4\tau_0^2 [y^2 + (E_c/G_c)x^2]} \right\}^{1/2} \quad (9)$$

Assuming $R \rightarrow 0$ in the disturbed zone, the unity within the brace may be neglected and at the very tip of the crack the total stress may be written as

$$\sigma = \sigma_0 \left\{ 1 + \frac{2\tau_0}{\pi\sigma_0} (E_c/G_c)^{1/2} \times \ln \frac{C\sigma_0}{2\tau_0 [y^2 + (E_c/G_c)x^2]^{1/2}} \right\} \quad (10)$$

This solution demonstrates that a singularity in front of a crack is weaker than in the Kolosov–Ingliš solution and, respectively, the dependence of reinforced composite strength on a crack length is not so sharp as in the Griffith criterion.

Equation 9 is analogous to the McClintock solution [11], found on the basis of results for planar yielding in front of a crack. Functions in front of logarithms in the Equation 9 and the McClintock solution coincide, although the functions under the log differ.

Equation 9 allows calculation of the stress concentration factor in the undestroyed element nearest to the crack in a one-dimensional layer composite. Assuming in Equation 10 that $y = 0$, the stress may be averaged on the element area

$$\langle \sigma \rangle = \frac{1}{H} \int_0^H \sigma(x) dx = K\sigma_0 \quad (11)$$

where H is the length of one layer of fibres with matrix. If $N = C/H$ (the number of destroyed fibre layers) Equation 11 yields

$$K = 1 + q \ln(Ne/\pi q) \quad (12)$$

$$q = \frac{2\tau_0}{\pi\sigma_0} (E_c/G_c)^{1/2} \quad (13)$$

The McClintock solution leads to the following expression for the stress concentration factor, K

$$K = 1 + q \ln(Ne/q^2) \quad (14)$$

Substituting experimental values of 0.14 and 0.06 for q in Equations 12 and 14 we obtain, respectively

$$K = 1.25 \text{ (Equation 12), } K = 1.69 \text{ (Equation 14)}$$

$$\text{for } q = 0.14 \text{ and } N = 1$$

$$K = 1.16 \text{ (Equation 12), } K = 1.40 \text{ (Equation 14)}$$

$$\text{for } q = 0.06 \text{ and } N = 1$$

Equation 14 leads to an obvious overestimation of the stress concentration factor which cannot be higher than 1.50. If the stress of the fractured layer is conveyed to two adjacent elements only, K will just equal 1.50. But Equation 14 leads to estimates of $K > 1.50$ if $q > 0.084$. Equation 12 does not have this shortcoming.

The stress concentration factor, K , is determined by two dimensionless parameters: the first, N , describes a crack length ($C = NH$ and H approximately equals the fibre diameter), the second, q , is defined by fibre and matrix properties (Equation 13).

It is natural to suppose that the crack growth starts if the stress in the fibres which are nearest to the crack tip reaches their strength, σ_f

$$\sigma = \sigma_f/K \quad (15)$$

Expanding K^{-1} in a power series of q , in the first approximation we obtain Equation 1. Thus, Equation 9 allows one to explain the log dependence of strength if the tangent of the slope of the straight lines in Figs 2 and 4 coincide with the coefficient in front of the logarithm (Equation 13).

3.3. Comparison of theory and experiment

To calculate the theoretical values of the coefficient in front of the logarithm, four parameters must be known: the composite tensile strength, σ_0 ; tensile Young's modulus, E_c ; the shear modulus, G_c ; and the matrix yield stress, τ_0 . Composite strength was determined by mechanical testing of rings, the tensile Young's modulus was calculated from the equation $E_c = V_f E_f$, where V_f and E_f are fibre volume content and modulus. The composite shear modulus was measured experimentally by torsion of unidirectional tubes with a fibre content of 65 to 68 vol %. The most serious problem lies in the determination of the matrix shear yield stress, τ_0 , in the composite. τ_0 may be obtained by

1. the measurement of matrix tensile yield stress, σ_1 , and consequent calculation from the equation

$$\tau_0 = \sigma_1/2 \quad (16)$$

$$\sigma_1 = 86 \text{ to } 92 \text{ MPa}, \quad \tau_0 = 43 \text{ to } 46 \text{ MPa};$$

2. the adhesion strength measurement based on the well-known fibre pull-out method. The adhesion strength of epoxy EDT-10 resin to the surface of the fibres is 100 ± 20 MPa [20]. If the yield limit of the matrix is lower, cohesive fracture of the resin will take place at a shear stress, τ_0 . Thus τ_0 must be > 80 to 120 MPa;

3. the measurement of composite shear strength which in glass fibre-reinforced plastic reaches 70 to 80 MPa [21].

The values obtained by methods 2 and 3 are not in conflict, but there is a contradiction with estimate 1. If the matrix yield limit is 45 MPa, the adhesion and composite shear strength will not be so high. During testing of thin resin films, yielding occurs in shear and it is not constrained due to the presence of the free surfaces. In cases 2 and 3 yield is constrained by the fibre, resulting in an increase in yield.

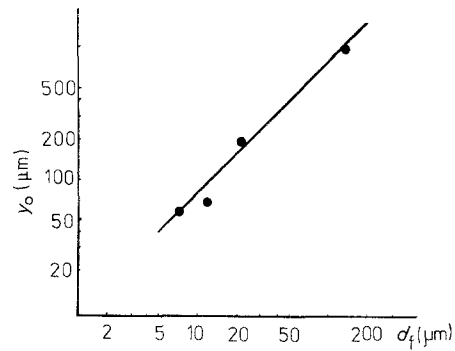


Figure 8 Dependence of the yield zone length, y_0 , on the broken glass fibre diameter, d_f .

To obtain the matrix yield stress in the composite by direct experiments, the dependence of the yield zone length near a broken fibre, y_0 , was measured optically in polarized light, and τ_0 was defined from the Kelly equation [18]

$$\tau_0 = \sigma d_f/4y_0 \quad (17)$$

where d_f is the fibre diameter, σ the fibre tensile stress.

The results are presented in Figs 8 and 9. According to Fig. 9 τ_0 is 110 ± 20 MPa and the matrix yield stress increases in the composite due to the fibre constraint effect. To calculate the theoretical value of the coefficient in front of the logarithm for glass fibre-reinforced plastic in Equation 13, values of σ_0 , τ_0 , E_c and G_c of 2.0 GPa, 110 MPa, 59 GPa and 6.5 GPa were used. The 0.11 value obtained is only 1.3-fold lower than the experimental value of 0.14.

To calculate q for organic fibre-reinforced plastic it is necessary to take into account that shear and transverse properties of polymer PABI fibres are lower than that of the epoxy EDT-10 resin [22]. For this reason, an increase in matrix yield stress in the composite is hardly possible, and composite yield stress is also determined by fibre properties. In this case, the fibre yield stress in Equation 13 must be substituted. For PABI fibres, the precise τ_0 value is not known. According to Andreev *et al.* [22] the PABI fibre shear strength is 40 to 60 MPa and according to Bazhenov *et al.* [23] the shear yield stress of PABI fibre-reinforced plastic is 40 to 50 MPa. Thus we may suppose $\tau_0 = 40$ to 50 MPa. Substituting into Equation 13 values for σ_0 , τ_0 , E_c and G_c equal to 2.2 GPa, 40 to 50 MPa, 72 GPa and 1.5 to 2.0 GPa, q is estimated to be 0.07 to 0.10. The experiment gives $q = 0.06$. Consequently, the coincidence between theory and experiment in both cases is satisfactory.

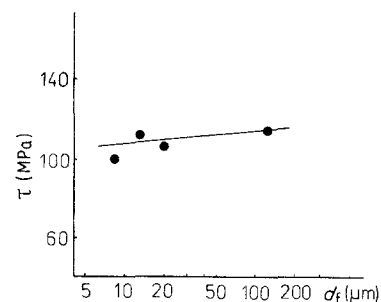


Figure 9 Dependence of the matrix shear yield stress in the composite on the broken glass fibre diameter, d_f .

4. Analysis

4.1. Effect of matrix on composite tensile strength

If the matrix yield stress is increased, the stress concentration near a defect grows (Equation 13). If all the fibres are equal in strength (σ_f), the composite failure criterion is attainment of σ_f in the fibres nearest to the defect (Equation 15). The existence of fibre strength dispersion leads to some complications in the problem. In this case, an increase in matrix yield stress leads to two mutually opposite effects. First, is the growth of stress concentration near defects and second is an increase in mean fibre strengths, σ_f , due to a decrease in fibre ineffective length.

To analyse composite strength dependence on τ_0 , the composite is considered to be a row of fibre layers connected by a matrix (Fig. 7). If N fibre layers are cut by a crack, their load is redistributed on to the unbroken fibres. The fibres in the layer nearest to the cracked layer receive an additional load $\Delta F = (K - 1)\sigma$, where K is the stress concentration coefficient and σ is the external stress. Owing to the stress concentration, the weakest fibres of the first layer break, and ΔF is reduced to $PK\sigma$, where P is part of the broken fibres. If the total additional load of the first layer of fibres ($\Delta F = (K - 1)\sigma - PK\sigma$) equals zero, crack growth begins.

For the Weibull distribution of fibre strength, this part of broken fibres is described by

$$P = 1 - \exp[-(K\sigma/\sigma_f)^b/b] \quad (18)$$

where σ_f is the fibre strength in the composite

$$\sigma_f = (ab\delta_0)^{-1/b} \quad (19)$$

where a and b are the Weibull distribution parameters [16], δ_0 is the fibre ineffective length, which is equal to double yield zone length, y_0 (Equation 17). Expanding the exponent into a series, as a first approximation we obtain

$$\sigma_c = [(K - 1)b/K]^{1/b} \sigma_f/K \quad (20)$$

The coefficient $[(K - 1)b/K]^{1/b}$ accounts for the fibre strength scattering. As it is approximately unity, the effect of fibre strength scattering on composite strength is not very significant.

Fig. 10 shows the dependence of glass fibre-reinforced plastic strength (Equation 20) on τ_0 .

If the defect length is not high ($N \leq 1$) the increase in τ_0 leads to a monotonic strength growth. The dependence is essentially different if $N \geq 2$. In this case, the strength maximum at some τ_0 value is observed.

At low matrix strength the stress concentration may be neglected and the failure mode is statistical accumulation of fibre breaks [16]. On the other hand, if the matrix strength is high, the stress concentration near the defects cannot be neglected, and the failure is by brittle growth of a crack.

We must note that the position of the maximum in Fig. 10 shifts if the defect length changes. The higher the defect size, the lower the yield stress matrix used must be to obtain maximum composite strength. This conclusion must be taken into account if the samples

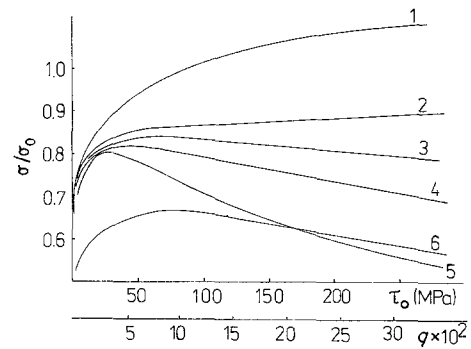


Figure 10 Dependence of glass fibre-reinforced plastic strength on matrix shear yield stress and q . (1) $b = 12$, $N = 0$; (2) $b = 12$, $N = 1$; (3) $b = 12$, $N = 2$; (4) $b = 12$, $N = 4$; (5) $b = 12$, $N = 20$; (6) $b = 6$, $N = 20$.

are tested with the aim to choose the matrix for a composite used in large-scale constructions. Note some increase in composite strength occurs with a decrease in b if τ_0 is too high. Thus in brittle composites, broadening of the fibre strength distribution decreases the danger of brittle failure to some extent.

According to Equation 13, matrix yield stress growth, increasing Young's modulus of the fibre, decrease in fibre strength and Young's modulus of the matrix lead to composite embrittlement. For example, the brittle failure of carbon fibre-reinforced plastic is more probable in comparison with glass fibre-reinforced plastic, due to the high Young's modulus of the carbon fibres. In metals, embrittlement is observed if the strength is increased; in reinforced composites the situation is opposite. For example, the progress in carbon fibre engineering resulting in an increase of fibre strength may decrease the danger of brittle fracture.

The effect of the matrix on composite strength may be investigated by changing the test temperature. It is well known that polymers are plasticized and their yield limit is reduced if the temperature is increased.

4.2. Effect of matrix plasticization on composite strength

Fig. 11 shows the variation of strength of aramid PPTA fibres and PPTA fibre-reinforced plastic with temperature. The fibre strength is reduced if the temperature is increased. On the contrary, the composite ring strength increases up to the matrix glass temperature (80°C). Of course, composite strength is reduced sharply above the matrix glass temperature,

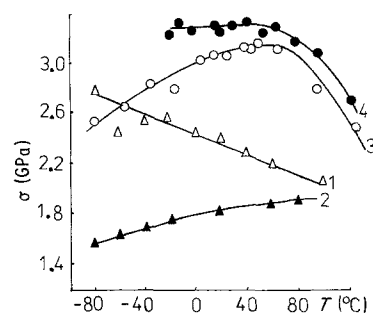


Figure 11 Temperature dependence of PPTA fibre-reinforced plastic strength. 1, filament of PPTA fibres; 2, ring samples; 3, flat cross-section strand; 4, round cross-section strands.

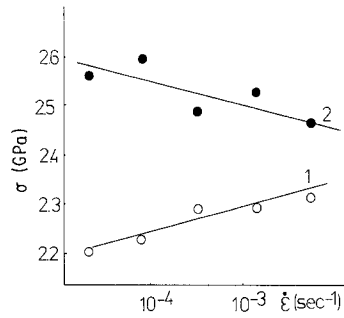


Figure 12 Dependence of strength of PPTA filament (1) and flat cross-section strand (2) on strain velocity.

due to its dramatically reduced properties. An increase in composite strength may be explained by a decrease in stress concentration near defects at elevated temperatures.

The strength of strands with round cross-sections is reduced monotonically if the temperature is increased. The effect may be explained by absence of defects in the samples. The strength of strands with a flat cross-section is maximum. These samples are very thin (four to five fibre diameter in thickness), and the fracture of a single fibre may lead to significant stress concentration in the unbroken neighbouring fibres. This may be the reason for the significant difference in temperature strength dependences of flat and round cross-section strands. The strength dependence of flat strands is analogous to that of ring samples.

Usually it is considered that different test methods result in similar dependences. Fig. 11 shows that this is wrong and even the shape of the strength curves may be different.

Fig. 12 shows the dependence of aramid fibre-reinforced plastic strength on strain velocity. The dependence is abnormal and increasing strain velocity leads to a decrease in composite strength despite increasing fibre strength.

Fig. 13 shows the effect of matrix plasticization. The epoxy resin was plasticized by increasing the diethylene glycol (DEG) modifier content. Plasticization leads to an increase in strand strength if the cross-section of the samples is flat.

The abnormal effects of temperature and strain velocity on strength may be explained by a decrease in stress concentration near defects with decreasing matrix yield stress.

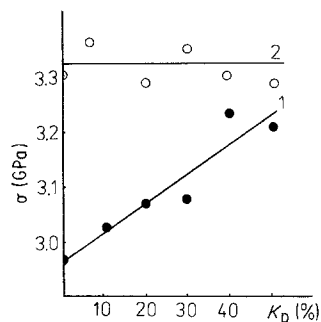


Figure 13 Variation of strength of PPTA fibre-reinforced strands with modifier DEG content in epoxy ED-20 matrix. 1, flat cross-section strand; 2, round cross-section strand.

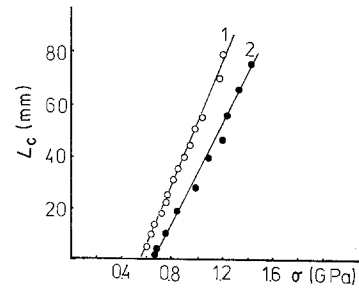


Figure 14 Length of longitudinal cracks appearing near a circular hole of 3 mm diameter plotted against tensile stress. 1, Glass fibre-reinforced plastic; 2, PABI fibre-reinforced plastic.

4.3. Longitudinal cracking near stress concentrators

Local shear deformation in the yield zone of the matrix is very high. For this reason, near a stress concentrator, four cracks oriented along the fibre direction may appear in the yield zone (Fig. 7) [7, 24, 25].

Fig. 14 shows the dependence of length of the longitudinal cracks appearing near a circular hole on the tensile stress. The cracks appear at critical stress, σ_0 . To find σ_0 the energy consideration may be used and the Griffith criterion in this case is valid [24]

$$\sigma_0 = (4G_{IIC}E_c/D)^{1/2} \quad (21)$$

where G_{IIC} is the shear fracture energy, E_c Young's modulus of the composite, and D the hole diameter.

According to Equation 21, longitudinal cracking is possible if the defect length exceeds D_c

$$D_c = 4G_{IIC}E_c/\sigma_0^2 \quad (22)$$

where σ_0 is the composite strength. The increase in fracture energy G_{IIC} and decrease in σ_0 lead to growth of the critical defect length, D_c .

If $D < D_c$ longitudinal cracking is not possible and the above theory is applicable to composite fracture. Thus fracture is a competition between two processes. The first is growth of the initial defect across the fibres due to stress concentration near it, and the second is longitudinal cracking. Longitudinal cracking is described by the Griffith criterion and is typical for long defects. Substituting typical values of G_{IIC} (Fig. 15), E_c and σ_0 for organic and glass fibre-reinforced plastics into Equation 22, we estimate $D_c \approx 0.5$ mm.

According to Equation 21, the shear crack must grow steadily to infinite length if $\sigma = \sigma_0$. In fact, the growth of longitudinal crack length leads to significant fracture energy increase (Fig. 15) due to the presence of unbroken fibre stringers which connect the

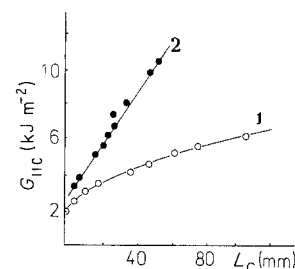


Figure 15 Fracture energy G_{IIC} plotted against length of longitudinal crack, L_c . 1, Glass fibre reinforced plastic; 2, PABI fibre-reinforced plastic.

opposite sides of the crack [25]. As a result, the energy is dissipated on fracture in the crack tip and also on work against shear forces due to the presence of stringers.

5. Discussion

Plastic zones appear at the tip of cracks in metals and isotropic polymers. Nevertheless, the Griffith criterion is applicable to polymers, but not to fibre-reinforced plastics. The main difference between these materials is the high anisotropy of the composite leading to a proportionality between the lengths of the yield zone and the crack. The fracture energy is proportional to the size of the plastic zone [26]. In epoxy resin, the critical length and thickness of the zone do not depend on crack length and, as a consequence, the fracture energy does not depend on crack length. In composites the yield zone length increases with growth of the crack length, the fracture energy is not constant and the Griffith criterion is not valid.

It should be noted that Equation 9 describes the stress distribution near a circular hole. The length of the plastic zone which appears near the hole is described by

$$y_0 = D\sigma_0/2\tau_0 \quad (23)$$

where D is the hole diameter. The boundary conditions for the hole problem coincide with the crack problem boundary conditions if $D = C$. Consequently, the stress distribution in the vicinity of the hole may be described by Equation 9. The composite is thus practically insensitive to the stress concentrator shape. It is interesting to note that in the present approximation there is a stress singularity near the hole.

The dependence of shear fracture energy on crack length (Fig. 15) is associated with the presence of unbroken fibres connecting the opposite sides of the crack. The stringers load the peeling composite strip with shear forces. If the shear stress, τ_s , does not depend on the distance from the crack tip, it is analogous to the matrix yield stress and Equation 9 may be used to describe the stress distribution near a defect for composites with elastic matrices. Thus τ_s is substituted for the matrix yield stress, τ_0 , in Equation 9. In fact, in glass fibre-reinforced plastic, τ_s cannot be considered constant due to the developing fracture of brittle glass stringers which leads to a decrease in τ_s , and G_{IIC} asymptotically approaches its limiting value at high crack length (Fig. 15). On the contrary, in PABI fibre-reinforced plastic, τ_s may be considered constant and Equation 9 may be used.

Transition from brittle failure to accumulation of fibre breaks may explain some abnormal effects. The first is an increase of carbon fibre-reinforced plastic residual strength after several cycles of preliminary loading and after impact [27]. Owing to a significant increase in yield zone length after preloading [28], an effective shear stress near defects is reduced. As a result the stress concentration is also reduced. The second is an increase of B/AI and glass fibre-reinforced plastics strength if the adhesion between fibre and matrix is degraded [29, 30]. The third effect is the abnormal temperature and strain velocity dependences

of strength in Figs 11 and 12. According to Kimura *et al.* [31] the C/C composite strength is maximum at elevated temperatures when the carbon matrix becomes plastic. It should be especially noted that the maximum position shifts to the region of higher temperatures for specially notched samples, compared to unnotched ones. The effect may be explained by the shift of maximum position in Fig. 10. Reduction of composite sensitivity to defects at elevated temperatures was demonstrated directly by Bazhenov *et al.* [32]. In glass fibre-reinforced plastic, the coefficient q decreases if the temperature is increased [32]. Of course, the temperature dependence of the maximum composite strength is not observed in all composites. For example, the strength of PABI fibre-reinforced plastic ($q = 0.06$ only) monotonically decreases [33].

It must be noted that there is a second effect leading to an increase in composite strength if the matrix is plasticized (at elevated temperatures, for example). In composites with high fibre elongation due to Poisson's contraction during loading, longitudinal cracking may appear. This leads to some strength decrease [34]. Matrix plasticization suppresses the cracking and a strength increase may also be observed [23, 34] for this reason.

6. Conclusions

1. Unidirectionally reinforced composite strength reduces logarithmically with increasing transverse crack length.
2. In samples without an artificial notch, defects already exist with their length depending on the fabrication process.
3. The stress distribution near a crack tip in a composite with an elastic-plastic matrix possesses logarithmic singularity.
4. The stress concentration grows with increasing matrix yield stress and Young's modulus of the fibre as well as with reduction in fibre strength and Young's modulus of the matrix.
5. Increasing matrix yield stress leads to composite embrittlement and a decrease in strength if the matrix yield is too high. The position of the strength maximum depends on defect length.
6. Matrix shear yield stress in the composite increases 2.0 to 2.5 times due to the fibre constraint of matrix yielding, compared to the yield of thin films.
7. Epoxy EDT-10 resin plasticization leads to increase in strength of aramid PPTA fibre-reinforced plastic.
8. Long cracks turn and grow along the fibre direction.

References

1. I. G. V. KOLOSOV, in "About One Application of Complex Variables Theory to Plain Problem of Mathematical Elasticity Theory" (Yuriev University, Yuriev, 1909) (in Russian).
2. A. A. GRIFFITH, *Phil. Trans. Roy. Soc. Ser. A* **221** (1921) 163.
3. S. W. TSAI and H. T. HANH, in "Inelastic Behavior of Composite Materials", presented at 1975 ASME Winter Annual Meeting, Houston, Texas, 30 November, edited by

- C. T. Herakovich, AMD, Vol. 13 (ASME, New York, 1975) Ch. 3.
4. C. W. SMITH, *ibid.*, Ch. 6.
 5. J. W. MAR and K. J. LIN, *J. Compos. Mater.* **11** (1977) 405.
 6. G. CAPRINO, *J. Mater. Sci.* **18** (1983) 2269.
 7. B. W. ROSEN, S. V. KULKARNI and P. V. McLAUGHLIN, in "Inelastic Behavior of Composite Materials", Presented at 1975 ASME Winter Annual Meeting, Houston, Texas, 30 November, edited by C. T. Herakovich, AMD Vol. 13 (ASME, New York, 1975) Ch. 2.
 8. H. V. BERGMANN, in "Carbon Fibers and Their Composites", edited by E. Fitzer (Springer-Verlag, Berlin, 1985) p. 184.
 9. S. L. BAZHENOV *et al.*, *Dokl. Akad. Nauk SSSR* **277** (1984) 854.
 10. R. PRABHAKARAN, *Mater. Sci. Engng* **41** (1979) 121.
 11. M. A. WRIGHT, in "Proceedings of the 1975 International Conference on Composite Materials", Vol. 1, edited by E. Scala, E. Anderson, J. Toth and B. R. Noton (AIME, New York, 1976) p. 866.
 12. F. A. McCLINTOCK, 4th Symposium on High Performance Composites, St Louis, 1969.
 13. P. M. SCOP and A. S. ARGON, *J. Comp. Mater.* **3** (1969) 30.
 14. G. I. KUDRIAVTSEV *et al.*, *Him. Volokna* **6** (1974) 70 (in Russian).
 15. G. A. BUDNITSKII, *ibid.* **2** (1977) (in Russian).
 16. B. W. ROSEN and N. F. DOW, in "Fracture", Vol. 7, "Fracture of Nonmetals and Composites", edited by H. Liebovitz (Academic Press, New York and London, 1972) Ch. 5, p. 300.
 17. V. A. VONSIATSKII *et al.*, *Compos. Mech.* **1** (1982) 9.
 18. A. KELLY, *Proc. Roy. Soc. Ser. A* **282** (1964) 63.
 19. L. I. MANEVICH, A. V. PAVLENKO and S. G. KOB-LIK, in "Asymptotic Method in Elasticity Theory of Orthotropic Body" (Visshaja Shkola, Kiev, 1981) p. 153.
 20. G. D. ANDREEVSKA, J. A. GORBATKINA and V. G. IVANOVA-MUMZHIEVA, *Phys. Chem. Mech.* **9** (1983) 3 (in Russian).
 21. A. M. KUPERMAN, W. G. IVANOVA and J. A. GOR-BATKINA, in "Vortrage II Wissenschaftlich Technische Tagung", Verstarbte Plaste-86, Dresden, 1986 (Dresden, 1986) G7/1 (in German).
 22. A. S. ANDREEV *et al.*, *Khim. Volokna* **3** (1983) 47.
 23. S. L. BAZHENOV *et al.*, *Sov. Phys. Chem.* **303** (1988) 1155.
 24. J. A. KIES, in "Prediction of Failure Due to Mechanical Damage in the Outer Hoop Winding in Fiberglass Pressure Vessels", Naval Research Laboratory, Rep. N5736 (Washington, 1962).
 25. A. A. BERLIN, V. A. TOPOLKARAEV and S. L. BAZHENOV, in "Physical Aspects of Fracture and Deformation of Heterogeneous Materials", edited by A. M. Leksovskii (FTI, Leningrad, 1987) p. 102.
 26. A. A. BERLIN *et al.*, *Visokomol. Soed Ser. A* **27** (1985) 1463 (in Russian).
 27. W. CANTWELL, P. CURTIS and J. MORTON, *Composites* **14** (1983) 301.
 28. S. L. BAZHENOV and A. A. BERLIN, *Sov. Phys. Chem.* **283** (1985) 1386.
 29. M. X. SHORSHOROV, L. E. GUKASIAN and L. M. USTINOV, in "Fracture Physics of Composite Materials" edited by A. M. Leksovskii and O. F. Kireenko. (FTI, Leningrad, 1979) p. 34.
 30. S. EGUSA *et al.*, *J. Nucl. Mater.* **119** (1983) 146.
 31. S. KIMURA, E. YASUDA and Y. TANABE, in "Proceedings of the 4th International Conference on Composite Materials", ICCM-IV Tokyo, October 1982, Vol. 2, edited by T. Hayashi, K. Kawata and S. Umekawa (The Japanese Society for Composite Materials, Tokyo, 1982) p. 1601.
 32. S. L. BAZHENOV *et al.*, in "Fracture Mechanics and Strength of Heterogeneous Materials", edited by A. M. Leksovskii (FTI, Leningrad, 1985) p. 154.
 33. L. V. PUCHKOV, A. M. KUPERMAN and E. S. ZEL-ENSKII, in "Proceedings of the 3rd Soviet Conference on Composite Materials" (Institute of Mechanics of Arm. SSR Academy of Sciences, Erevan, 1979) p. 28 (in Russian).
 34. E. F. KHARCHENKO *et al.*, *Compos. Mech.* **2** (1987) 345.

*Received 25 April
and accepted 20 October 1989*